JOURNAL OF MATERIALS SCIENCE 25 (1990) 3017–3023

Gas-induced damage in elastomeric composites

B. J. BRISCOE, S. ZAKARIA
Chemical Engineering Department, Imperial College, Exhibition Road, London SW7, UK

Gases may induce extensive and irreversible damage in elastomers when they are allowed to escape from the polymeric matrix. The damage is most evident as internal lacerations and also as an overall change in certain mechanical properties. The damage process, commonly termed explosive decompression failure, is really confined to gas-polymer systems which are initially equilibrated at high pneumatic stresses; greater than 10^7 Pa. Two interrelated facets of this phenomenon are described in the context of elastomeric composites with particular emphasis on the role of interfacial quality. The results of an optical examination of the internal cracks found during a typical gas-induced rupture cycle are described. The system is a commercial silicone elastomer–glass filler composite where the fillers have been surface modified in order to alter the adhesive strength of the interface. The data indicate that the filler particles significantly modify the stress fields in the elastomer during gas-induced rupture. Essentially, the fillers suppress the development of the characteristic large scale axially symmetrical stress fields in the composites. This visual assessment of the damage is then related to the deterioration in certain mechanical properties of this current system.

1. Introduction

Elastomeric materials are known to absorb significant quantities of gas at high ambient pressures [1–4] which produce proportionally higher equilibrium gas mass sorption. Accompanying the sorption, which may or may not induce swelling of the elastomer, there is evidence that the polymer is also under a net hydrostatic stress [2, 3]. The ambient pressure thus produces high environmental triaxial stresses on the system and a high gas concentration in the polymer. The state of the polymer–gas mixture at equilibrium is not known, but it is assumed that a uniform concentration and stress fields are developed.

The rapid release of the ambient pneumatic pressure surrounding a saturated specimen often results in the production of extensive internal and external surface ruptures. The damage process is frequently referred to as explosive decompression failure. It is known that the polymer mass fractures internally at some stage after the ambient pressure is reduced [4–8]. For example, unfilled cylindrical samples develop a series of axially symmetrical cracks at apparently well-defined times during the decompression history. Spherical samples similarly produce centre symmetrical spherical cracks [4]. The mechanistic details of the processes responsible for this type of damage are not developed in fine detail but the available experimental evidence is consistent with the following model. It is supposed that the elastomer fails in local hydrostatic tension; this is not the only available stress field capable of inducing failure but it has the virtue of analytical precedent. Materials fracture internally in negative hydrostatic tension or pressure at small volumetric strains because the stored energy can be easily expended to create new surfaces, i.e. cracks, in the system. However, even large positive hydrostatic pressures do not damage elastomeric systems [9]. Gent and co-workers [10–12] used a local hydrostatic tension failure criterion for the treatment of this type of problem. In addition, it is speculated here that the hydrostatic tension arises from two sources. As the prevailing gas concentration is progressively reduced the gas diffusing out of the sample produces a gas concentration gradient in the sample. The changing concentration gradients create effective hydrostatic stress gradients and, as a result, local volumetric changes occur in the specimen. The triaxial tension due to the expansion of the ambient gas also creates an additional and complementary supposed uniform body stress in the sample. The magnitudes of these stresses are probably defined by the gas concentration–volume characteristics of the gas–polymer solution. Once the gas-induced cracks have developed, they are inflated by the gas which desorbs into these cavities from the adjacent matrix. Surface blisters and cleavage cracks may also appear during this process in certain elastomeric systems depending upon the permeability of the test specimen [4]. Elastomers more resistant to gas permeation tend to retain a significant volumetric swelling and density changes for a significant length of time after the rapid gas depressurization is completed [8]. In a particulate composite under such a tensile field, the stresses in the matix are transferred to the filler in two ways: through shear stress at the matrix–filler interfaces and through components of the tensile stresses at the interfaces. The filler particles become stress centres. In a specimen saturated with gas, competitive adsorption of gas molecules at the filler–matrix interfaces may also tend to weaken the matrix–filler interfacial bonds [13]. During decompression,

0022-2461/90 $03.00 + .12

when the negative stresses reach a critical level, the weakly bonded fillers may become detached from the elastomeric matrix and readily form vacuoles. This phenomenon is called dewetting [11]. The vacuoles grow, in part by inflation, into the elastomer and failure of the matrix results. On the other hand, particles that remain firmly bonded to the matrix may also be stress raisers but do not become nuclei for crack initiation [14]. In these systems the initial failures appear to take place within the elastomer near the inclusions and not at the interface. This failure mode is termed cavitation [11, 12].

Gent and Tompkins [10] have investigated these types of initiation and crack growth for unfilled and filled elastomeric systems. The study on filled systems was restricted to the application of quasi-triaxial tension using uniaxial body forces and not gas-induced stresses. They do, however, suggest that the quasi-triaxial tension produced by uniaxial stresses is equivalent to the pressurizing of the interior of an elastomeric sample using a gas-induced stress field. The cracks, it was suggested, would initiate from pre-existing voids or flaws and they proposed that the matrix failure would occur when the triaxial tension reached a critical stress of $5/2G$, where G was the shear modulus. The cracks would then grow in an unstable fashion if this value of the triaxial stress was maintained.

The present paper examines the influence of rigid fillers on the explosive decompression process with particular emphasis upon the effect of the quality of the filler–matrix interface. Low concentrations of the glass spheres have been used in conjunction with a transparent silicone elastomer. The interface quality has been modified and separately characterized. The study is in two parts. An optical examination and characterization of the gas desorption-induced crack pattern is described and analysed. The paper also describes a series of mechanical deformation studies on gas-induced damaged samples. Here, the trends in certain mechanical properties have been used in an attempt to deduce the extent and nature of the internal crack damage.

2. Experimental techniques and apparatus

2.1. Specimen preparation

A transparent and colourless elastomer, polydimethylsiloxane (Dow Corning, Brussels, Sylgard 184) has been used as the matrix to facilitate the optical examination of the gas-induced damage in the specimens. The Young's modulus of the elastomer was ~ 1.2 MPa. The glass beads (Jencons & Co., Bedfordshire), in the diameter range of 60 μm, were used as the filler. The beads were washed with dichloromethane prior to use. Various surface modifications were undertaken to both increase and reduce the matrix–filler adhesion.

The interfacial bonding between the glass beads and the elastomer was improved by treating the clean beads with a 10% solution of dichlorodimethylsilane in dichloromethane solvent. Similarly, surfaces were also modified with a special adhesion promoter (Dow Corning, Primer 92-023). In addition the glass beads were treated with a 5% solution of a solid silicone resin (GE Silicones, New York, SR 350) in toluene to reduce the polymer–filler interaction. Smooth glass plates of comparable composition were also treated in a similar way to provide specimens for model matrix–filler adhesion studies involving a blister test (see below).

The composite specimens were prepared by mixing 100 parts Sylgard S-184 silicone polymer with 10 parts Sylgard C-184 curing agent by weight. The surface-modified fillers were added to the mixture to prepare the different specimens. The filler quantity in each case was 0.5% by weight of the mixed elastomer. The mixture was then degassed under vacuum (50 mtorr) for ~ 30 min. The vacuum was frequently broken to facilitate removal of trapped air. The liquid polymer was then cast into cylindrical moulds (25 mm diameter and 100 mm high). Flat circular sheets of the clear elastomers, were also cast (3 mm thick and 100 mm diameter) on to the surface-modified glass plates for the blister test (see below). The moulds were stored at room temperature for 7 d. Pronounced settling of the filler particles was not observed during the cure time.

2.2. Interface characterization

Blister test experiments were performed to quantify the effect of the surface chemical treatments on the interface quality. In a blister test a pre-existing hole at the interface was pressurized by a constant flow of gas. Gas pressure and the height of the bubble formed were measured and recorded on a microcomputer. Details of this experimental method have been given elsewhere [15]. The data from the blister test were analysed using the expression given by Briscoe and Panesar [15]. The value of the fracture energy was calculated as a function of crack velocity; Fig. 1. The values of fracture energy for the interfaces treated with the adhesion promoters were significantly higher than those for the untreated interface which in turn

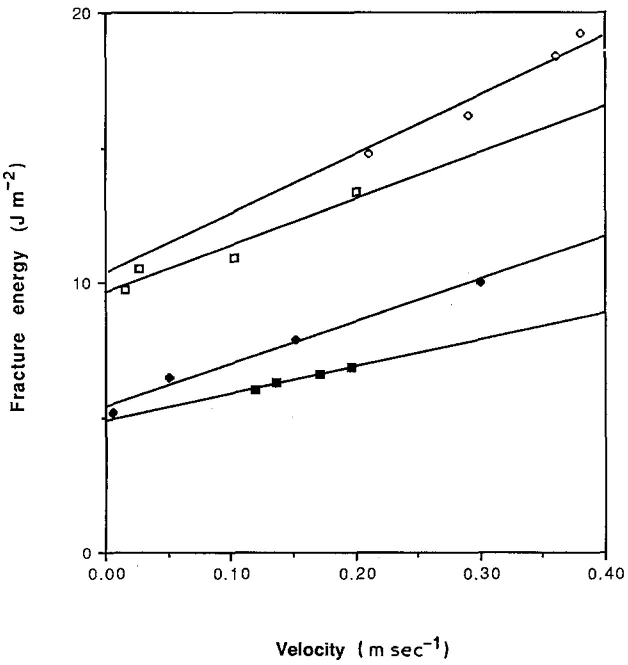

Figure 1 Interfacial fracture energy as a function of crack velocity for various interfaces. (◇) Primer (× 5), (□) silated, (◆) untreated, (■) release.

TABLE I Fracture energy at a crack velocity of 0.2 m sec^{-1}

Specimen type	Fracture energy (J m^{-2})
Release	6.5
Untreated	8.5
Silated	12.8
Primer	72.0

was greater than that found for the plates treated with the release agent. For comparison purposes, Table I lists the fracture energy value of the various interfaces at a crack velocity of 0.2 m sec^{-1} which has been arbitrarily chosen as the reference velocity.

2.3. Stress generation equipment

The pressure vessel assembly consisted of a stainless steel pressure vessel, 610 mm long with an o.d. 127 mm and an i.d. 50.8 mm. A compressed air-driven reciprocating gas pump (Charles Madan, Altincham, UK) was used to pump the CO_2 gas. An intermediate gas receiver was used between the compressor and the pressure vessel to dampen pressure fluctuations during pressurization. The gas pressure was released manually through a 3 mm needle valve. A more detailed description of the equipment used and its operation are given elsewhere [16]. The vessel containing the prepared specimens was heated to a temperature above the critical temperature of CO_2 (45° C) and was pressurized to ~21 MPa. The gas pressure was maintained for ~3 h so that the specimens were completely saturated with the CO_2 gas and a quasi-equilibrium condition was achieved. The gas pressure was released from 21 MPa to ambient in ~90 sec.

3. Assessment of the damage in the specimens

3.1. Optical methods

Thin cross-sections (1 mm) of the damaged specimens were cut on a low-speed cutting wheel (Buehler, UK). The specimens had been previously cast in an epoxy resin to facilitate this cutting process. These thin sections were soaked in a commercial black ink to highlight the cracks in the transparent matrix. Fig. 2 shows typical photographs of these cross-sections. The crack patterns in various thin cross sections were analysed using an image analyser (OMS Optimax V, Cambridge). The number of cracks, the mean crack length and the percentage of cracked area in each cross-section of the damage specimen are given in Table II. The sections of various damaged specimens were also examined and photographed under an interference microscope (Carlzeiss Jena, East Germany) and with a scanning electron microscope (Joel, T200A), Fig. 3.

TABLE II Optical assessment of damage in various specimens

Specimen	Crack area (%)	Crack number	Mean length (mm)
Clear	8.5	79	10.5
Clean filler	18.4	146	7
Release	25	255	6
Silated	28	207	3
Primer	30	128	3

3.2. Mechanical methods

The damaged composite specimens were studied in three ways in an attempt to quantify the extent of the overall gas-induced damage.

1. Simple diametric compression of cylindrical samples (length-to-diameter L/D ratio $\simeq$ 1) at 20° C, Fig. 4.
2. Cyclic diametric compression of cylindrical samples ($L/D \simeq 1$) at 20° C, Fig. 6.
3. Sinusoidal (3 Hz) tensile deformation of the rectangular specimens (maximum strain 250 μm) in the temperature range 30 to 80° C, Fig. 7.

4. Results and discussion

4.1. Optical method

The visual inspection of the damaged specimens soon after (~10 min) their exposure to the described explosive decompression cycle, did not reveal any apparent surface blisters or noticeable increase in their volume. Surface blisters and an increase in the volume of nitrile rubbers have been reported in explosive decompression. The nitrile rubber specimens revert to their original volume and the surface blisters disappear after the absorbed gas has completely escaped (~24 h) [4]. The permeability of CO_2 gas in polydimethylsiloxane rubber is relatively high and has been reported to be 325 × 10^{-9} cm^3 (STP).cm.sec^{-1} cm^2.cm Hg [17], as compared to nitrile rubber which has a lower value of 3 × 10^{-9} cm^3 (STP).cm sec^{-1}.cm^2. cm (Hg) [8]. We can thus say that this silicone elastomer system had more rapidly reverted to its original dimensions.

The number of cracks, mean crack lengths and percentage areas of the cracks in different sectioned specimens are given in Table II. Two distinctly different types of crack were observed. The large and axially symmetrical circular cracks near the surface were detected in all the samples. Briscoe and Liatsis [4] have also observed similar circular cracks in their work on explosive decompresion of commercial seal materials. In addition, smaller and rather randomly oriented internal cracks are also visible in the matrices. These cracks were probably generated by the overall triaxial expansion of the specimen that occurs due to the negative hydrostatic pressure produced inside the test piece in the course of a rapid decrease of the ambient pressure. The large axially symmetrical cracks are mainly oriented in circumferential planes and do not produce large crack-area contributions in the visual analysis. The smaller randomly oriented cracks make a proportionally larger contribution. The specimen with no filler particles, had the smallest number of cracks and also had the lowest crack area in the cross-section.

In the absence of filler particles, the mean crack length was comparatively large. The most notable feature is that the introduction of fillers, irrespective of the interface quality, increases the number of cracks observed. The presence of the rigid inclusions seems to produce an effect similar to that observed and

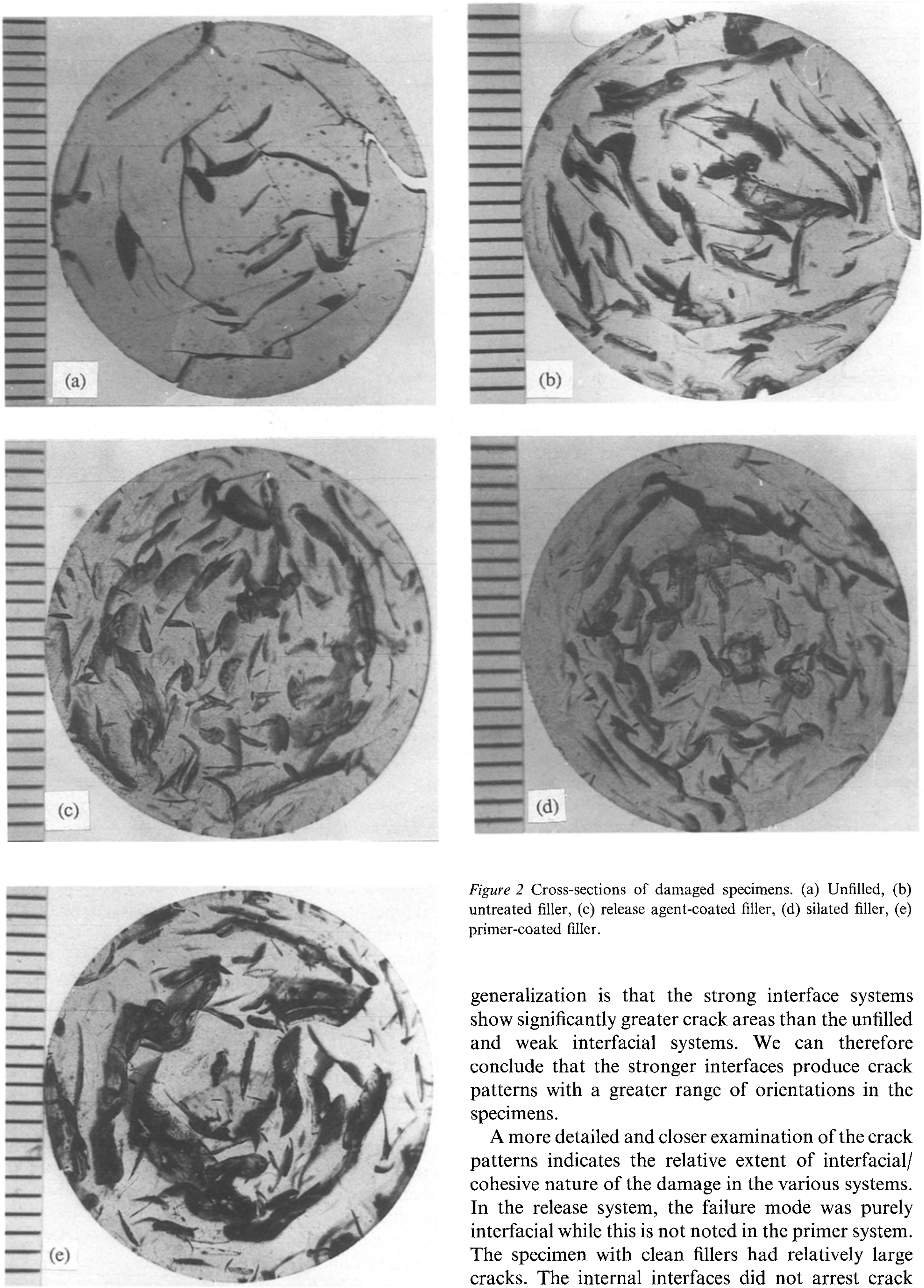

Figure 2 Cross-sections of damaged specimens. (a) Unfilled, (b) untreated filler, (c) release agent-coated filler, (d) silated filler, (e) primer-coated filler.

described by Gent and Lindley [18]. They axially strained thin sheets of rubber which were firmly bonded to rigid metallic plates. In the thinnest test piece a large number of small cracks was detected and, as the test piece thickness increased, the average crack size became larger and their number decreased. A second generalization is that the strong interface systems show significantly greater crack areas than the unfilled and weak interfacial systems. We can therefore conclude that the stronger interfaces produce crack patterns with a greater range of orientations in the specimens.

A more detailed and closer examination of the crack patterns indicates the relative extent of interfacial/cohesive nature of the damage in the various systems. In the release system, the failure mode was purely interfacial while this is not noted in the primer system. The specimen with clean fillers had relatively large cracks. The internal interfaces did not arrest crack growth and were debonded when they came across an approaching crack. The filler particles sometimes also appear to dewet and initiate cracking, Fig. 3a. In the specimen with the release agent coated fillers, the particles were mostly at the centre of the cracks, Fig. 3c. The wedge shape of these cracks on either side of the filler particles, indicated that the fillers had been the nucleating site for these cracks. In this system,

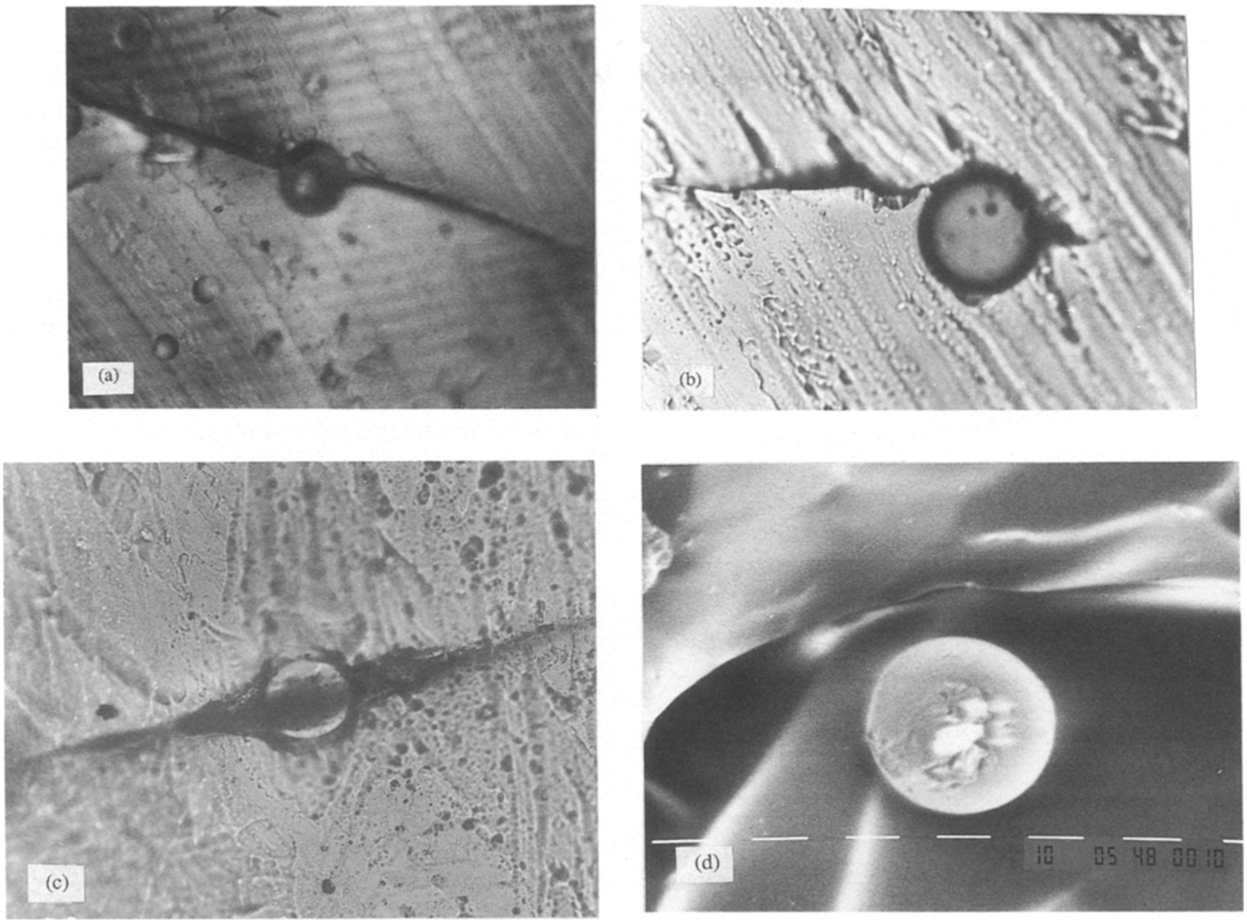

Figure 3 (a) Interfacial rupture of an untreated clean interface, (b) crack arrested at strong interface, (c) crack initiated at an interface treated with release agent, (d) scanning electron micrograph of an interface treated with a primer.

although the number of cracks was maximum, the individual sizes of the cracks were relatively small. Under the high ambient gas pressure it seems that the gas became sorbed at the weak interfaces around the filler particles. During the gas decompression a vacuole is easily formed at the interface which inflated into the matrix and generated new surfaces. This process relieves the large negative triaxial stresses acting upon the specimen and also facilitates the rapid desorption of the absorbed gas in the matrix. This

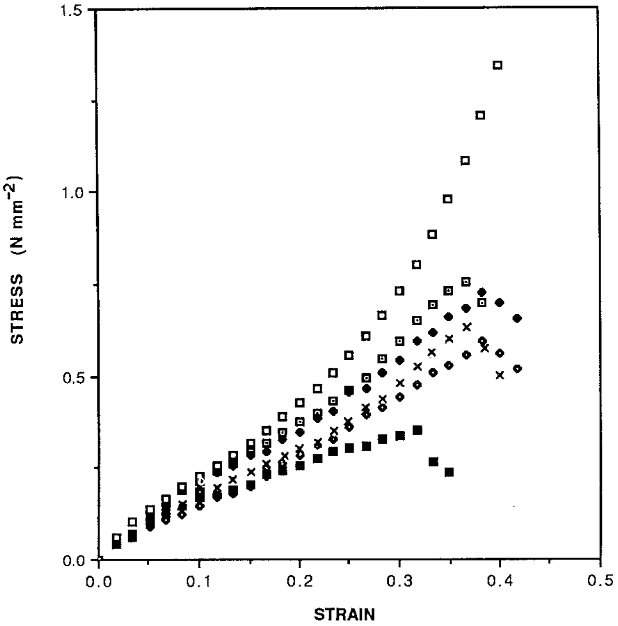

Figure 4 Stress as a function of lateral strain for various specimens: (■) unfilled, (◇) with untreated filler, (x) with release agent-coated filler, (◆) with silated filler, (□) with primer-coated filler, (□) undamaged clear specimen.

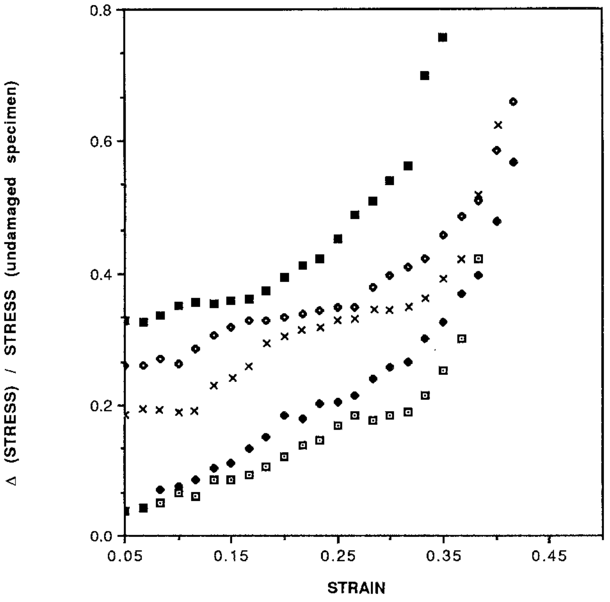

Figure 5 Normalized stress as a function of lateral strain for various specimens: (■) unfilled, (◇) with untreated filler, (x) with release agent-coated filler, (◆) with silated filler, (□) with primer-coated filler.

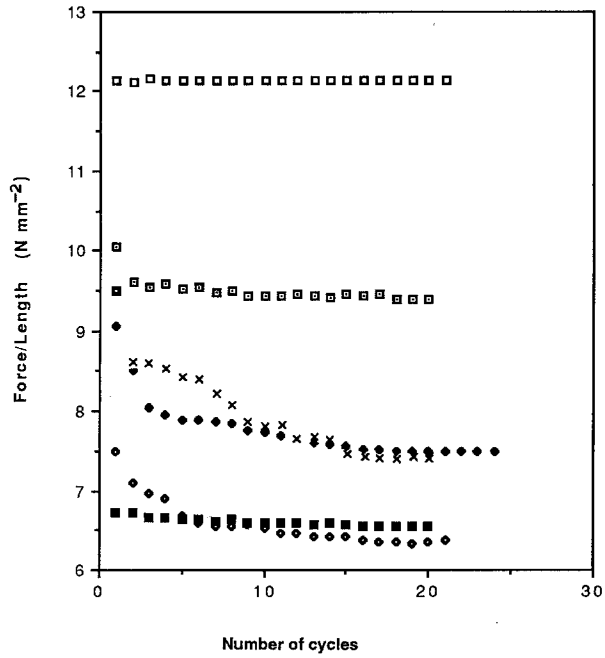

Figure 6 Change in the force required for 30% lateral strain as a function of cyclic loading of various specimens: (■) unfilled, (◇) with untreated filler, (◆) with release agent-coated filler, (x) with silated filler, (□) with primer-coated filler, (□) undamaged specimen.

prevents unstable crack growth. The appearance of the system with the strong interfaces is consistent with no dewetting during the rapid decompression. The silated interfaces either arrested the cohesive crack growth or changed its direction, Fig. 3b. The modified filler surfaces formed strong bonds with the elastomeric matrix resulting in a tough layer of polymer around the filler. The high-pressure penetrating gas was unable to corrupt the interfaces and the matrix remained attached to the filler particles during depressurization. This is evinced by the fact that cavitation of the matrix occurred rather than dewetting of the filler particle. The failure surfaces were rough and also the elastomer was not completely removed from the filler surface. A scanning electron micrograph of such interfaces is given in Fig. 3d. The estimated number of cracks in this system was low.

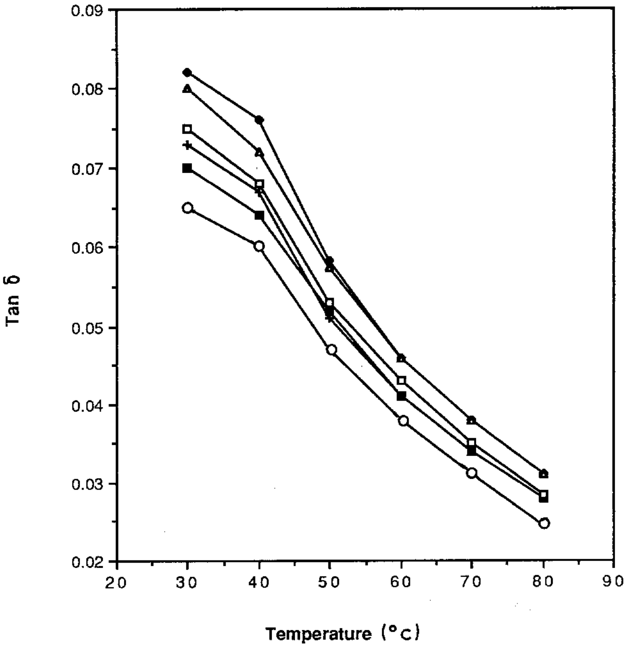

Figure 7 Loss tangent of various specimen of temperature: (◆) unfilled, (△) with untreated filler, (□) with release agent-coated filler, (+) with silated filler, (■) with primer-coated filler, (○) undamaged clear specimen.

4.2. Mechanical properties of damaged samples

The general sensitivity of the various systems to explosive decompression damage is apparent from Fig. 4, which shows the compressive stress against lateral strain for a range of samples. The reference sample of an undamaged silicone elastomer indicates the elastic response of a crack-free matrix. The reduction in the modulus is a reflection of the extent of internal crack development and possibly crack orientation. Fig. 5 provides a more succint ranking where the stress difference compared to the undamaged sample is plotted against strain. The form of the plots is similar for each sample although the absolute values of the normalized stress difference at a given strain are dissimilar. Table III gives the value of the normalized stress difference at 20% strain for comparison purposes. Reference to Table I shows that there is quite a good correlation between the loss of stiffness of the gas-induced damaged composites and the inverse of the interface quality as indicated by the interfacial fracture energy measured in the blister test.

The transverse compressive experiment described above produces a range of compressive and tensile fields in the sample. An indication of the extent of the additional crack growth induced by the transverse stress is apparent from Fig. 6, which shows the behaviour of the various damaged test specimens in cyclic loading. Two systems appear to be rather insensitive to additional crack propagation: the strongest interface and the unfilled system. These samples are those with the least number of observed cracks; Table II. The fatigue sensitivity actually scales quite well with the crack number; the release-coated system is the most sensitive and in addition has the highest crack population; Table II.

The viscoelastic loss characteristics of the damaged samples provide similar data to the force–displacement characteristics described. Fig. 7 is a summary of various data. The cyclic strain opens and closes the cracks and the additional viscoelastic loss is presumably associated with the dissipation of internal crack peeling energy. The magnitude of this work will be related to the total crack area and the geometric disposition of the cracks. The work will be a function of the crack number and their length. The major stress

TABLE III Normalized stress at 20% lateral strain

Specimen	Normalized stress
Clear	0.4
Clean filler	0.32
Release	0.3
Silated	0.18
Primer	0.12

divertors will be radial and here the axially symmetrical cracks will be the most active. We deduced earlier that the mean axial symmetry will be inversely related to the crack area sensed in the axis of the sample (projected axis area). Thus we observe a relationship between the magnitude of the measured loss and the inverse of the axially sensed crack area.

In brief, the mechanical characteristics of damaged samples indicate that the extent of the gas-induced damage scales apparently with the interfacial quality of the matrix–filler interface and that the unfilled system is the most vulnerable to damage.

5. Conclusions

This study has shown that the presence of filler particles within an elastomeric matrix significantly modifies the nature and extent of the internal rupture produced when the rubber is exposed to gas desorption-induced rupture or explosive decompression failure. The effect of the filler particles is generally to suppress the large-scale axially symmetrical stress fields which lead to the formation of large but relatively few cracks which occur in the unfilled system. These cracks normally follow the stress field symmetry and are also axially symmetrical. We have been able to distinguish in detail the effect of the interfacial quality on the failure mechanism during decompression. Weak interfaces promote dewetting of the particle–matrix interface in the dynamic gas desorption stress field and also these lesions act as inflation centres. The filler particles which have strong interfaces with the matrix induce cavitation failures in the matrix away from the interface. In both cases the fillers have the effect of producing what appears to be a more homogeneous local stress environment in the elastomer. Not only is the mean crack size decreased but the crack number increases as does the randomness of the crack orientation.

The second part of the paper establishes a correlation between the gas-induced damage and the change in certain mechanical properties. It has been common to use such a mechanical evaluation to quantify the extent of explosive decompression-induced damage. The three mechanical tests described are shown to be good indicators of the extent of damage, as deduced from the optical examination. A very sensitive estimate of the extent of damage is obtained from a measurement of the loss properties of the damaged system. We also note in passing that a system's resistance to explosive decompression failure, as sensed by changes in mechanical properties, is improved by the introduction of fillers where there is a strong bond between the filler and the matrix. These systems fail by the creation of a multitude of small cavities in the matrix which, as a matter of experiment, cause the least loss of the composite's coherence.

References

1. G. K. FLEMING and W. J. KOROS, *Macromol.* **19** (1986) 2285.
2. M. R. EUDES *et al.*, *Nucl. Eng.* **6** (1968) 586.
3. D. H. ENDER, *J. Chemtech.* **16** (1986) 52.
4. B. J. BRISCOE and D. LIATIS, *J. Polym. Sci.* to be published.
5. D. COOK, paper no. 19, PRI Discussion Forum and Exhibition on "Offshore Engineering with Elastomers", Aberdeen, Scotland, 5–6 June 1985.
6. A. D. GRIFFTHS, paper no. 20, *ibid.*
7. D. J. POTTS, paper no. 21, *ibid.*
8. H. A. WOLCOTT and S. R. STRAZNICKAS, Energy Sources Technical Conference and Exhibition, ASME Petroleum Division, Dallas, Texas, 17–22 February 1985, p. 157.
9. G. H. LINDSEY, *J. Appl. Phys.* **38** (1967) 4843.
10. A. N. GENT and D. A. TOMPKINS, *J. Polym. Sci. A2* **7** (1969) 1483
11. A. N. GENT and BYOUNGKYEU PARK, *J. Mater. Sci.* **19** (1984) 1947.
12. K. CHO and A. N. GENT, *ibid.* **23** (1988) 141.
13. L. E. LAWRENCE, *J. Macromol. Sci.* **A1** (1967b) 929.
14. G. SALOMON and F. VAN BLOOIS, *J. Appl. Polym. Sci.* **8** (1964) 1991.
15. B. J. BRISCOE and S. S. PANESAR, *J. Phys. D* **19** (1986) 841.
16. H. MAGHEREFTEH, PhD thesis, Imperial College (1983).
17. E. L. WARRICK *et al.*, *Rubber. Chem. Tech.* **52** (1978) 437.
18. A. N. GENT and P. B. LINDLEY, *Proc. Roy. Soc. (London)* **A249** (1959) 195.

Received 9 May
and accepted 12 September 1989